MCB
Journals.ASM.org

The B55α Regulatory Subunit of Protein Phosphatase 2A Mediates Fibroblast Growth Factor-Induced p107 Dephosphorylation and Growth Arrest in Chondrocytes

Victoria Kolupaeva, Lea Daempfling,* Claudio Basilico

Department of Microbiology, New York University School of Medicine, New York, New York, USA

Fibroblast growth factor (FGF)-induced growth arrest of chondrocytes is a unique cell type-specific response which contrasts with the proliferative response of most cell types and underlies several genetic skeletal disorders caused by activating FGF receptor (FGFR) mutations. We have shown that one of the earliest key events in FGF-induced growth arrest is dephosphorylation of the retinoblastoma protein (Rb) family member p107 by protein phosphatase 2A (PP2A), a ubiquitously expressed multisubunit phosphatase. In this report, we show that the PP2A-B55α holoenzyme (PP2A containing the B55α subunit) is responsible for this phenomenon. Only the B55α (55-kDa regulatory subunit, alpha isoform) regulatory subunit of PP2A was able to bind p107, and this interaction was induced by FGF in chondrocytes but not in other cell types. Small interfering RNA (siRNA)-mediated knockdown of B55α prevented p107 dephosphorylation and FGF-induced growth arrest of RCS (rat chondrosarcoma) chondrocytes. Importantly, the B55α subunit bound with higher affinity to dephosphorylated p107. Since the p107 region interacting with B55α is also the site of cyclin-dependent kinase (CDK) binding, B55α association may also prevent p107 phosphorylation by CDKs. FGF treatment induces dephosphorylation of the B55α subunit itself on several serine residues that drastically increases the affinity of B55α for the PP2A A/C dimer and p107. Together these observations suggest a novel mechanism of p107 dephosphorylation mediated by activation of PP2A through B55α dephosphorylation. This mechanism might be a general signal transduction pathway used by PP2A to initiate cell cycle arrest when required by external signals.

The response of cells to growth factor signaling is often cell type specific, so that different cells exposed to the same growth factor will show a totally different biological response ranging from stimulation of proliferation, differentiation, or growth inhibition. While in some cases this could be due to the utilization of distinct, although cognate receptors, in many other cases it can be shown that different biological outcomes result from activation of the same receptor in a different biological context.

An example of such behavior is the response of chondrocytes to fibroblast growth factor (FGF) signaling. Chondrocyte proliferation and differentiation are required for the process of endochondral ossification that mediates the formation and growth of long bones and vertebrae. One of the major regulators of this process is FGF signaling. Excessive or unregulated FGF signaling caused by activating FGF receptor (FGFR) mutations strongly inhibits chondrocyte proliferation and affects their differentiation, resulting in several bone morphogenetic disorders (1), and it is now quite clear that the major biological response of chondrocytes to FGF is inhibition of cell proliferation.

This response is cell type specific and contrasts with the proliferative FGF response in most other cells. We have sought to identify the determinants of the growth inhibitory response of the chondrocytes to FGF, and we previously showed (2) that it required the function of the p107 and p130 members of the retinoblastoma protein (Rb) family but not of pRb (3). Rb proteins are vital cell cycle regulators, and their function is regulated by phosphorylation at several Ser/Thr residues. In the active hypophosphorylated form, Rb proteins interact with and inhibit transcriptional activation by the E2F family of transcription factors that control the expression of many cycle progression genes. Phosphorylation by cyclin-dependent kinase (CDK)/cyclin complexes inactivates the Rb proteins, allowing E2F factors to positively influence cell cycle progression (4).

Consistent with the growth inhibitory response, Rb proteins all become dephosphorylated upon FGF treatment of chondrocytes, but while p130 and pRb undergo dephosphorylation several hours after exposure of the cells to FGF, p107 is dephosphorylated within the first hour of FGF treatment. p107 dephosphorylation is observed in the presence of RNA and protein synthesis inhibitors, indicating that it results from a signaling event (5). The finding that p107 dephosphorylation occurred while chondrocytes still exhibited robust activity of CDK/cyclin complexes suggested that it resulted from the activation of a phosphatase (5, 6), and we showed that p107 dephosphorylation was both an early and key event in the induction of growth arrest produced by FGF in chondrocytes and required the activity of protein phosphatase 2A (PP2A).

PP2A is an abundant Ser/Thr phosphatase which represents a family of 4 dimeric and >90 heterotrimeric holoenzymes. The phosphatase consists of a scaffolding, structural A subunit (PR65) which forms a stable complex with the catalytic C subunit. This heterodimer in turn associates with a regulatory B subunit that

Received 27 December 2012 Returned for modification 16 January 2013
Accepted 11 May 2013
Published ahead of print 28 May 2013

Address correspondence to Victoria Kolupaeva, Victoria.Kolupaeva@nyumc.org, or Claudio Basilico, claudio.basilico@med.nyu.edu.

* Present address: Lea Daempfling, Institut für Biologie, Berlin, Germany.

doi:10.1128/MCB.01730-12

determines substrate specificity and subcellular localization and comprises at least 4 families of molecules with over 20 members (7). A variety of studies have demonstrated that PP2A regulates a number of cellular processes. It is also generally regarded as a tumor suppressor, as PP2A predominantly displays proapoptotic functions (8–11).

The complexity of PP2A activity regulation is highlighted by the fact that its functions can be regulated in different ways: through interaction with inhibitory proteins, such as cancerous inhibitor of PP2A (CIP2A) (12) and simian virus 40 (SV40) small t antigen (13), through modifications of the catalytic subunit (7) and by complexing with different regulatory subunits. A variety of substrates specific for different regulatory subunits have been reported, yet the way in which they are specifically targeted by PP2A is often not understood. Moreover, the same regulatory subunit might target a set of diverse substrates. For example, the B55α (55-kDa regulatory subunit, alpha isoform) subunit has been involved in dephosphorylation of CDK1/cyclin B1 substrates during the mitotic transition (14–16), dephosphorylation of AKT (Thr308) (17), Tau protein (18), FOXO1 (forkhead box O1) transcription factor (19), EDD (a negative regulator of p53) (20), beta-catenin (21), and p107 (22). The latter was also reported to be a substrate of PP2A-PR59 holoenzyme (23).

The work presented here aimed to identify the PP2A regulatory subunit whose activation by FGF results in p107 dephosphorylation and growth arrest of chondrocytes. We show that the B55α subunit is highly expressed in chondrocytes and is the only regulatory subunit that can stably bind p107. The association of B55α with p107 is increased by FGF treatment and knockdown of B55α blunts p107 dephosphorylation and the FGF growth-inhibiting response. The interaction of B55α with p107 requires the spacer region of p107 and appears to favor dephosphorylated over phosphorylated p107. Importantly, phosphorylation of B55α at several specific serine residues strongly inhibits its affinity to PP2A A/C dimers and eliminates p107 binding, in line with the finding that the B55α form that is coimmunoprecipitated with p107 in RCS (rat chondrosarcoma) cells is dephosphorylated. While the mechanisms by which FGF signaling "activates" the PP2A-B55α holoenzyme (PP2A containing the B55α subunit) to dephosphorylate p107 remains to be elucidated, dephosphorylation of the B55α subunit is likely responsible for the increase in PP2A phosphatase activity and/or affinity to p107 that lead to p107 dephosphorylation and the initiation of cell cycle arrest.

MATERIALS AND METHODS

Reagents and antibodies. All chemicals were from Sigma-Aldrich (unless otherwise stated). ATP was from New England BioLabs, [γ-^{32}P]ATP was from PerkinElmer, and Lipofectamine 2000 was from Life Technologies. The following antibodies were used: anti-PP2A-A (antibody against the alpha isoform of regulatory subunit A of PP2A) (H300), anti-PP2A-B55α (2G9), anti-p107 (C-18), and agarose-conjugated anti-p107 (Santa Cruz Biotechnology); anti-α-tubulin (clone B-5-1-2), antiactin, antibody against glutathione *S*-transferase (anti-GST), and antibody against hemagglutinin (anti-HA) (Sigma-Aldrich); antiphosphoserine, antiphosphothreonine, anti-phospho-pan (Life Technologies), anti-PP2A-A (07-250), and anti-PP2A-C (05-545) (EMD Millipore Corporation); anti-phospho-p44/42 mitogen-activated protein kinase (MAPK) (extracellular signal-regulated kinases 1 and 2 [ERK1/2]), anti-p44/42 MAPK (ERK1/2), anti-PP2A-B55α (100C1), anti-phospho-AKT (Ser473), anti-AKT (Cell Signaling Technology), and antistreptavidin (IBA BioTagnology). Protease and phosphatase inhibitor cocktails were purchased from Thermo Scientific, and restriction enzymes and T4 DNA ligase were purchased from New England BioLabs.

Cell culture and fluorescence-activated cell sorting (FACS) analysis. Rat chondrosarcoma (RCS), OB1, and $C_3H_{10}T1/2$ cells were maintained in Dulbecco modified Eagle medium (DMEM) supplemented with 10% fetal calf serum (FCS) at 37°C and 9% CO_2. For *in vivo* labeling with [^{32}P]orthophosphate (PerkinElmer), the cells were washed with phosphate-free DMEM and incubated for 6 h with the same medium containing 0.4 mCi of [^{32}P]orthophosphate/6-cm dish. Labeling was stopped by washing the cells twice with ice-cold phosphate-buffered saline (PBS). The cells were lysed in buffer A as described below. PP2A-A scaffolding PR65 subunit with the Strep-tag (IBA BioTagnology) fused to C terminus was amplified from the PR65–Strep-tag III (PR65-StrepIII) plasmid (51) and inserted into pBABEpuro vector between BamHI and EcoRI sites. The individual RCS cell clones were obtained by 2-week selection with puromycin. Retroviral vector expressing p107SC-FLAG was stably introduced into RCS cells (24). A PCR fragment from GST-p107SC for bacterial infection (22) was inserted between the EcoRI and BamHI sites in the pLXSN vector using the following primers: 5′-TATAGAATTCACCAUG GTTCCTACCTGTGAAGAA-3′ and 5′-TATAGGATCCTTACTTGTCA TCGTCATCCTTGTAATCATGATTTGCTCTTTCACTGAC-3′ (the sequence for the FLAG tag is underlined). The sequence contains amino acids V585 to N780 fused to Y949 to H1068. RCS cells with empty pLXSN vector were used as a control. The p107S-HA vector was obtained by inserting the PCR fragment from the GST-p107S construct (22) into the pUNO-mcs vector (InvivoGen) between the BamHI and PstI sites using the following primers: 5′-TATAGGATCCACCAUGGTTCCTACCTGT GAAGAAGTTATATTC-3′ and 5′-TATACTGCAGTTAAGCGTAATCT GGAACATCGTATGGGTAGTTTATTCCAGTTGAATGTACCTC (the sequence for the HA tag is underlined). Plasmids containing the sequence for mutations in the B55α subunit were generated using QuikChange site-directed mutagenesis kit (Agilent Technologies) according to the manufacturer's protocol. RCS cells were transfected with an equal amount of plasmids using Lipofectamine 2000 according to the manufacturer's instructions. Cells were treated with fibroblast growth factor (FGF1) (10 ng/ml) (a kind gift from M. Mohamadi, New York University [NYU]) and heparin (5 μg/ml) as indicated in the figure legends. Chondrocytes from the ribs of newborn rats were isolated in accordance with the standard procedure (25) and treated with FGF after 48 h for the periods of time indicated in the figures legends. 32 To induce oxidative stress, H_2O_2 (final concentration of 800 μM in PBS solution) was administered to the RCS cells for the periods of time indicated in the figure legends. Flow cytometry was performed using FACScan (Becton, Dickinson) and analyzed using ModFit LT (Verity Software House) software.

siRNA transfection. The small interfering RNA (siRNA) (sense and antisense strands) were purchased from Ambion (Life Technologies). The sense strand sequences were the following: siRNA B55α1, 5′-GGUUUAU CUAUGAAACGGA-TT; siRNA B55α2,5′-GAAAGAACUGGAACGCG AA-TT. Transfections were performed using Lipofectamine 2000 according to the manufacturer's instructions (Life Technologies). Cells were transfected twice with a 24-h interval between the two transfections to increase siRNA uptake. One hundred fifty picomoles of siRNAs was used for a 12-well plate. The cells were treated with FGF1 36 h after transfection for the periods of time indicated in the figure legends.

Immunoprecipitation, GST pulldown assay, and *in vitro* protein phosphorylation. Protein lysates were prepared in buffer A (50 mM Tris HCl [pH 7.4], 150 mM NaCl, 10 mM KCl, 1% NP-40, 1 mM EDTA) in the presence of phosphatase inhibitors (1 mM Na_3VO_4, 10 mM NaF,10 mM $Na_4P_2O_7$) and protease inhibitors (Halt protease inhibitor cocktail, EDTA-free; Thermo Scientific Inc.). For Strep-tag purification, okadaic acid (OA) (final concentration of 5 nM) was added to buffer A. For immunoprecipitation, 0.5 mg of total protein was incubated with 2 μg of antibody overnight at 4°C. Agarose-conjugated anti-p107 and anti-PP2A-Bα (2G9, supplemented with protein A/G Plus-agarose) antibodies were used. For detection of phosphorylated PP2A-Bα, cell lysates were

prepared using buffer A, and then 0.5 mg of total protein was incubated for 2 h at 4°C in the presence of 0.3% SDS to disrupt PP2A complexes. Anti-PP2A-Bα antibodies (2G9, supplemented with protein A/G Plus-agarose) were used overnight at 4°C. Glutathione-Sepharose 4B beads (20 μl of 50% suspension in PBS) were used to immunoprecipitate GST-tagged PP2A regulatory subunits (26). The immune complexes were washed 4 times with 1 ml of buffer A. Input (5%) from RCS cells and immunoprecipitates (50%) were resolved on 10% SDS-polyacrylamide gels and analyzed by immunoblotting. Anti-mouse IgG and anti-rabbit IgG were used as a negative control for p107 and B55α immunoprecipitates, respectively.

For GST pulldown assays, p107 mutants were isolated from bacteria using glutathione-Sepharose 4B. Bacterial cultures were centrifuged, resuspended in buffer B (50 mM Tris HCl [pH 7.4], 100 mM KCl, 0.1 mM EDTA, 0.1% Triton X-100, 5% glycerol) and sonicated. Sonicated bacterial lysates were then cleared by centrifugation and added to a glutathione-Sepharose 4B column. The bound material was washed with 10 volumes of GST buffer (50 mM Tris HCl [pH 7.4], 50 mM KCl, 1.5 mM DTT, 5% glycerol) and eluted with 20 mM reduced glutathione in GST buffer. Amicon Ultra filters (cutoff, 10 kDa) were used to concentrate eluted fractions and to reduce glutathione concentration to 1 μM. For GST pulldown assay, 20 to 50 pmol of GST-tagged p107 mutants were preincubated for 30 min at 4°C with 20 μl glutathione-Sepharose 4B beads, and then 0.3 mg of total cell lysate prepared in buffer A was added and incubated for 2 h at 4°C. The bead pellet was washed three times with 1 ml of buffer A. Boiled samples were then subjected to 10% SDS-PAGE. For GST pulldown assay with phospho- and nonphospho-p107 mutants, 230 pmol of GST-tagged p107 mutants was phosphorylated by cyclin E/CDK2 complexes (1 μg; Millipore) in the presence of 25 μCi [γ-^{32}P]ATP in the "kinase" buffer (50 mM HEPES [pH 7.4], 15 mM $MgCl_2$, 25 mM β-glycerophosphate, 2.5 mM EGTA, 1 mM dithiothreitol [DTT], 20 μM ATP) for 30 min at 30°C. The reaction mixtures were desalted using Zeba spin desalting column (Thermo Scientific) equilibrated with buffer A and supplemented with phosphatase inhibitors. The nonphosphorylated mutants were treated in exactly the same way with the enzyme omitted from the reaction mixture.

Large-scale Strep-tag purification. RCS cell lines expressing PR65-StrepIII were cultured as described above and treated with FGF1 for the periods of time indicated in the figure legends. Five 150-mm plates were used for a single time point. Hyaluronidase treatment (20 min at 37°C; final concentration of 250 units/ml) was combined with FGF treatment to facilitate cell lysis. The cells were washed twice with cold PBS and collected in buffer A supplemented with 5 nM OA. Thirty-five milligrams of total protein was loaded on the column packed with 200 μl of Strep-Tactin resin (IBA BioTagnology). The columns were washed twice with 20 volumes of buffer A supplemented with 5 nM OA, and complexes were eluted with buffer A (supplemented with 5 nM OA and 3 mM desthiobiotin, NP-40 omitted) in five 200-μl fractions. These fractions were concentrated on Amicon Ultra YM-10 units (Millipore) and loaded on gradient (8 to 12%) SDS-PAGE. The gel was stained with SimplyBlue SafeStain Coomassie blue stain (Invitrogen) compatible with mass spectrometry according to the manufacturer's protocol.

RESULTS

The majority of protein phosphatase 2A holoenzymes in RCS cells contain B55α or B56δ regulatory subunits. p107 dephosphorylation is a key event in FGF-induced cell cycle arrest in chondrocytes and is mediated by protein phosphatase 2A (PP2A) (27). However, the PP2A holoenzyme responsible for FGF-induced p107 dephosphorylation is unknown as well as the mechanism of FGF-induced PP2A activation. To identify the specific PP2A complex that mediates FGF-induced p107 dephosphorylation, we first determined the organization of PP2A heterotrimeric enzymes in rat chondrosarcoma (RCS) cells, using PR65 (A subunit, a scaffolding subunit) as bait. RCS cells were chosen for these experiments, as they exhibit most properties of proliferating chondrocytes, including the FGF inhibitory response.

Retroviral vector encoding PR65 (human, alpha isoform) fused to StrepIII at its C terminus was stably introduced into RCS cells. PR65-StrepIII protein can be easily distinguished not only by anti-StrepIII antibodies (Fig. 1A, bottom gel) but also by anti-PP2A-A antibodies due to the decreased electrophoretic mobility of the tagged PR65 subunit (Fig. 1A, top gel). Two clones with the highest levels of PR65 expression were chosen for further purification (lanes 1 and 3 in the top gel in Fig. 1A). The FGF response of both clones was identical to parental RCS cells as was confirmed by rapid p107 dephosphorylation and ERK1/2 activation (Fig. 1B). PP2A-PR65-StrepIII complexes Strep-PR65 subunit from FGF-treated or untreated cells were affinity purified on streptavidin agarose; eluates (Fig. 1A, bottom gel) were concentrated and separated on the gradient SDS-polyacrylamide gel (Fig. 1C). The protein bands of interest were identified by mass spectrometry. As expected, the major band with 33 matched peptides was assigned to the alpha isoform of the A subunit (Fig. 1C). PP2A-C catalytic subunit (both alpha and beta isoforms) was also identified in eluted complexes. Several regulatory subunits were detected. One of the most abundant bands was identified as regulatory B55 subunit, alpha isoform (B55α) (Fig. 1C). Out of 15 matching peptides, four could be also matched to the delta isoform (B55δ) with only one additional unique peptide (FFEEPEDPSSR) for B55δ. No unique peptides were identified for the B55β subunit, though it shares 6 matching peptides with B55α. The B' (B56) family of regulatory subunits was represented by B56ε, B56δ, and B56γ isoforms (Fig. 1C).

We were also able to identify several other proteins that copurified with the PR65 subunit and might be potential substrates of PP2A. Two proteins, eukaryotic elongation factor 1-alpha (eEF1A1; gi|28460696) and eukaryotic elongation factor 2 (eEF2; gi|33859492) are major components of the translation machinery (28). The activities of both proteins are modulated by phosphorylation; however, the phosphatase that would counteract their phosphorylation is not known (29–31). The presence of eEFA1 and eEF2 in PP2A complexes suggests that PP2A might be responsible for their dephosphorylation. PP2A has been implicated in modulation of phosphorylation status of acetyl-coenzyme A carboxylase (ACC) (32). Accordingly, this protein was detected in PP2A complexes (gi|11559962) (Fig. 1C). Among other detected proteins were γ-actin (gi|4501887) and α-actinin 4 (gi|77539778). Both proteins were mainly detected in FGF-treated cells but not in untreated RCS cells. It has been reported that actin phosphorylation was important for its functions (33). Thus, actin enrichment in PP2A complexes upon FGF treatment may reflect its functional interaction with PP2A which would counteract its phosphorylation, while α-actinin's presence is likely due to its stable binding to actin rather than direct binding to PP2A. FGF treatment of RCS cells causes strong cytoskeletal alterations (34; also our unpublished data), which might require changes in phosphorylation status of actin.

Since B55α and B56 family members were the most abundantly expressed PP2A regulatory subunits in RCS cells, we overexpressed the B55α regulatory subunit and 4 members of B56 family (α, δ, γ, and ε) to investigate their potential interaction with p107. Association of p107 with the B55α subunit has been previously reported in U2OS cells (22) under physiological conditions; however, it was not known whether this interaction is

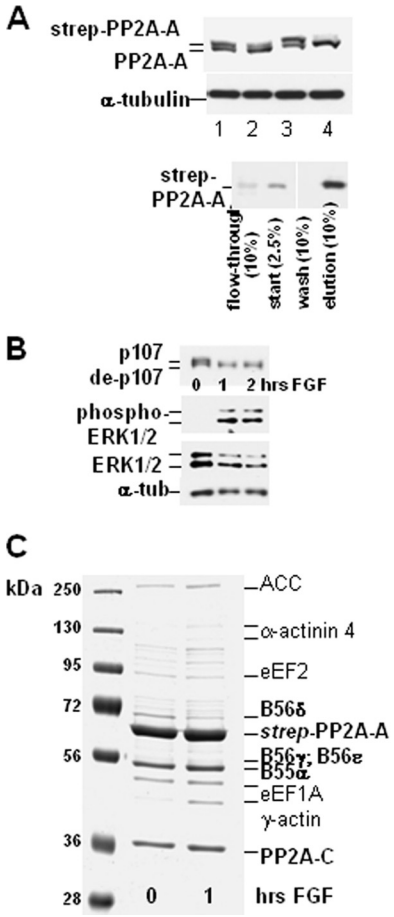

Summary of the proteins identified from PR65 Strep III complexes by mass spectrometry

Peptides matched	*NCBI accession number*	*Mol. mass*	*Protein description*
33	gi/8394027	65281	alpha isoform of regulatory subunit A, protein phosphatase 2 (PP2A-A)
57	gi/3342500	35611	Protein phosphatase 2A, catalytic subunit alpha isoform (PP2A-C α)
60	gi/18394024	35552	Protein phosphatase 2A, catalytic subunit beta isoform (PP2A-C β)
15	gi/16758910	52159	Protein phosphatase 2A, 55 kDa regulatory subunit, alpha isoform (PP2A-B55α)
5	gi/148747146	51973	Protein phosphatase 2A, 55 kDa regulatory subunit, delta isoform (PP2A-B55δ)
6	gi/16758910	51678	Protein phosphatase 2A, 55 kDa regulatory subunit, beta isoform (PP2A-B55β)
10	gi/7387498	55064	Protein phosphatase 2A, 56 kDa regulatory subunit, epsilon isoform (PP2A-B56ε)
22	gi/1022894 gi/7387500	66972 68332	Protein phosphatase 2A, 56 kDa regulatory subunit, gamma and delta isoforms (PP2A-B56γ, PP2A-B56δ);

FIG 1 Identification of functional PP2A multiprotein complexes in RCS cells. PR65-StrepIII (subunit A, a scaffolding subunit) was stably introduced into RCS cells, and these cells were treated with FGF for the periods of time (in hours) indicated in the figure. (A and B) Twenty micrograms of total protein from the indicated cell lines (clones 1 to 4 overexpressing PR65-StrepIII) was analyzed by SDS-PAGE following by immunoblotting. Equal amounts of protein loading were confirmed by α-tubulin immunodetection. (A) Anti-PP2A-A antibodies identify two bands in the cell lines overexpressing PR65-StrepIII (endogenous/tagged). The top band is also recognized by anti-StrepIII antibody (bottom panel). Aliquots from each step of the purification (as indicated in the bottom panel) were analyzed by immunoblotting. (B) ERK1/2 is activated by FGF in experimental cell lines similar to parental RCS cells. de-p107, dephosphorylated p107; α-tub, α-tubulin. (C) Thirty-five milligrams of total protein from the cells overexpressing PR65-StrepIII was loaded on the Strep-Tactin resin, and PP2A PR65-StrepIII containing holoenzymes were isolated as described in Materials and Methods. After concentration, the final elutes were separated on gradient SDS-polyacrylamide gels and stained with SimplyBlue SafeStain Coomassie blue stain. The bands of interest were identified by mass spectrometry, and the corresponding proteins are indicated on the gel and in the table to the right (Mol. mass, molecular mass). The subunits of PP2A are indicated by bold type.

preserved in other cell types and whether these proteins also interact upon FGF treatment.

Interaction of the B55α subunit of PP2A with p107 is FGF sensitive and important for mediating the FGF inhibitory response. To investigate the interaction between p107 and different PP2A regulatory subunits, we ectopically expressed GST-tagged B subunits in RCS cells treated with FGF or not treated with FGF (Fig. 2A, left panel) (26). Overexpression of the different regulatory subunits did not alter the intracellular concentration of PP2A-A and C subunits (data not shown) and was not affected by FGF treatment. To identify a regulatory subunit that is able to bind p107, we immunoprecipitated p107 from RCS cells and determined whether an association between endogenous p107 and a regulatory subunit was induced by FGF treatment. Figure 2A (right panel) shows that the only regulatory subunit detectable in p107 immunoprecipitates was B55α. This binding was increased in FGF-treated RCS cells. Similar results were obtained in 293 cells (Fig. 2B), supporting our hypothesis that the interaction between p107 and B55α is not cell type specific. However, this interaction is FGF sensitive in RCS cells but not in 293 cells, which have very low levels of FGF receptors (Fig. 2A and B, right panels). To confirm our findings, GST-tagged B regulatory subunits were pulled down, and immunoprecipitates were assayed for the presence of p107. p107 was detected only in B55α immunoprecipitates (Fig. 2C and data not shown) in RCS and 293 cells. In line with our previous data, this interaction was stimulated by FGF in RCS cells (Fig. 2C). As expected, PP2A-A and C subunits were also detected or recovered in GST immunoprecipitates (Fig. 2C). Consistent with our previous report (27), the increase in association of PP2A with p107 induced by FGF was transient, as association was less detectable at later times of treatment. These results indicate that PP2A-B55α holoenzymes are likely responsible for mediating FGF-induced p107 dephosphorylation in chondrocytes.

To further support our findings, we measured the interaction between endogenous B55α and p107 in RCS cells. p107 was immunoprecipitated from untreated or FGF-treated RCS cells, and

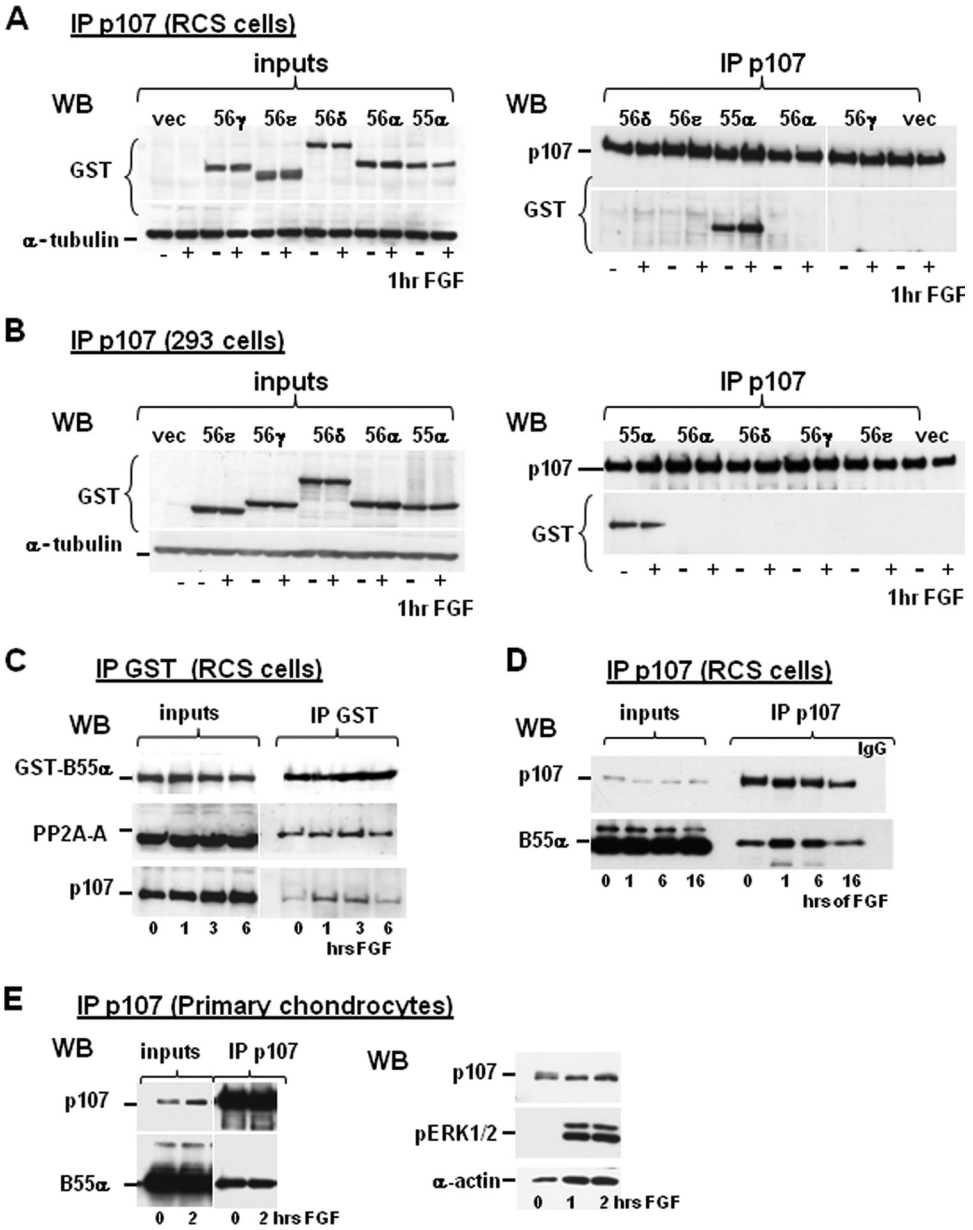

FIG 2 FGF induces an association between B55α and p107. (A and B) GST-tagged B regulatory subunits were transiently overexpressed in FGF-treated (+) or untreated (−) RCS (A) and 293 (B) cells (left panels). Twenty micrograms of total protein was analyzed by Western blotting (WB) using anti-GST antibody, and equal amounts of protein loading were confirmed by α-tubulin immunodetection. Lysates were normalized to the amount of total protein and subjected to immunoprecipitation (IP) with agarose-conjugated anti-p107 antibody (right panels). The presence of B subunits in p107 immunoprecipitates was assayed by GST antibodies. vec, vector. (C) GST-B55α was transiently overexpressed in FGF-treated or untreated RCS cells, and GST immunoprecipitates were analyzed by WB with anti-PP2A-A, anti-p107, and GST antibodies. (D and E) p107 interacts with endogenous B55α in RCS cells (D) and in primary chondrocytes isolated from newborn rats (E [left panel]). p107 immunoprecipitates from FGF-treated or untreated cells were analyzed with anti-p107 and anti-B55α antibodies. (E, right) FGF treatment caused rapid p107 dephosphorylation and ERK1/2 activation in primary chondrocytes. Twenty micrograms of total protein was analyzed by WB, and equal amounts of protein loading were confirmed by α-actin immunodetection. pERK1/2, phosphorylated ERK1/2.

the presence of B55α in immunoprecipitates was analyzed by specific antibodies. As shown in Fig. 2D, B55α was detected in p107 immunoprecipitates, and FGF treatment transiently increased the association between p107 and B55α.

While RCS cells represent an extensively used model for proliferating chondrocytes, it is important to demonstrate that p107 also interacts with the B55α subunit in primary chondrocytes. We therefore performed p107 immunoprecipitation in FGF-treated and untreated primary chondrocytes isolated from newborn rats. We have previously demonstrated that the FGF inhibitory response of primary chondrocytes is characterized by rapid p107 dephosphorylation and ERK1/2 activation (Fig. 2E, right panel) (27). The association between B55α and p107 was detected in FGF-treated and untreated primary chondrocytes (Fig. 2E, top

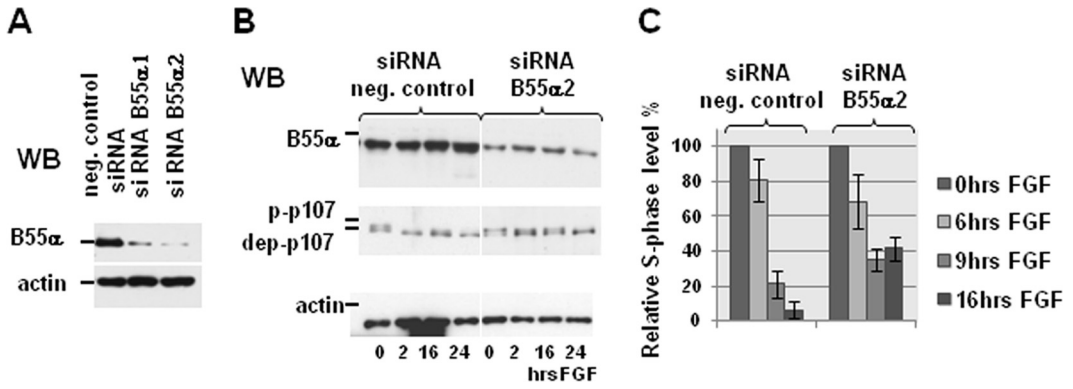

FIG 3 Knockdown of B55α subunit inhibits FGF-induced p107 dephosphorylation and growth arrest in chondrocytes. RCS cells were transfected with siRNAs (siRNA B55α1 and siRNA B55α2) against the B55α subunit or negative-control siRNA. (A) Both siRNAs caused significant reduction in B55α levels. Ten micrograms of total protein was analyzed by WB using B55α antibody. Equal amounts of protein loading were confirmed by α-actin immunodetection. (B) FGF-induced p107 dephosphorylation is delayed in RCS cells transfected with siRNA B55α2. Ten micrograms of total protein from FGF-treated or untreated RCS cells transfected with negative control (neg. control) or B55α2 siRNAs was analyzed by WB. Equal amounts of protein loading were confirmed by α-actin immunodetection. p-p107, phosphorylated p107; dep-p107, dephosphorylated p107. (C) FACScan analysis of RCS cells transfected with negative-control and B55α2 siRNAs and treated with FGF for the periods of time (in hours) indicated in the figure. The numbers on the *y* axis indicate the relative percentages of total cells in S phase. The data are representative of several independent experiments, and the values are means ± standard deviations (SD) (error bars).

gels). Together, our data indicate that PP2A-B55α holoenzyme interacts with p107 in chondrocytes and is likely responsible for FGF-induced p107 dephosphorylation.

To confirm this conclusion, we sought to knockdown B55α expression using RNA interference. We first infected RCS and 293 cells with lentiviral vectors expressing short hairpin RNAs for B55α to produce stable cell lines. The corresponding regions of B55α rat and human mRNAs were targeted; however, we were able to significantly reduce B55α expression only in 293 cells (data not shown). RCS cells appeared to be extremely sensitive to the level of B55α expression and were not able to sustain prolonged selection with antibiotic. To overcome this problem, RCS cells were transfected with siRNAs against the B55α subunit (Fig. 3A). Two different siRNAs, siRNA B55α1 and siRNA B55α2 described in Materials and Methods, caused substantial reduction (up to 85%) in B55α expression, while negative-control siRNA had no effect (Fig. 3A). Both siRNAs were used for further experiments. p107 was dephosphorylated within the first hour of FGF treatment in cells transfected with negative-control siRNA. In contrast, knockdown of the B55α subunit by siRNA B55α2 resulted in a substantial delay (up to 16 h) in p107 dephosphorylation (Fig. 3B, left panel). Cells with reduced levels of B55α initially responded to FGF treatment similar to control cells, bur at later times, they were clearly resistant to FGF-induced growth arrest with about 40% of the original level of S-phase cells compared to about 5% in the control cell line (Fig. 3B, right panel). Similar results were obtained with siRNA B55α1 (not shown). We therefore conclude that a PP2A holoenzyme containing the B55α subunit is required for the dephosphorylation of p107 and consequent growth arrest induced by FGF in chondrocytes.

The B55α subunit of PP2A preferably binds dephosphorylated p107. To further understand the mechanism of FGF-induced p107 dephosphorylation and the role of B55α in this process, we thought to counteract p107 dephosphorylation by overexpressing a deletion mutant of p107 that was still able to bind the B55α subunit. It has been shown in U2OS cells that the shortest p107 fragment that can bind the B55α subunit as efficiently as full-length p107 comprises the spacer region fused to the C-terminal domain (p107SC) (Fig. 4A) (22). The spacer region itself (p107S) had slightly lower affinity to B55α. We first determined whether the association between those mutants and B55α is preserved in RCS cells. RCS lysates were preincubated either with GST-tagged p107 mutants or GST protein purified from bacteria and then subjected to GST pulldown assay. As shown in Fig. 4B, both p107SC and p107S mutants were able to immunoprecipitate endogenous B55α subunit from RCS cells with comparable affinities. We therefore generated RCS cell lines constitutively expressing FLAG-tagged p107SC (FLAG-p107SC) mutant (Fig. 4C). Overexpression of p107SC did not change kinetics of endogenous p107 dephosphorylation (Fig. 4C) and had no effect on FGF-induced growth arrest (data not shown). We next overexpressed the shortest p107S HA-tagged mutant in RCS cells (Fig. 4D, inputs). As we expected, the B55α subunit was detected in HA-tagged p107S (HA-p107S) immunoprecipitates (Fig. 4D, left panel). To confirm these data, we immunoprecipitated the B55α subunit and were able to detect HA-p107S mutant copurified with the B55α subunit (Fig. 4D, right panel). Overexpression of the p107S mutant resulted in a delay of p107 dephosphorylation of up to 12 h and in partial resistance of cells to FGF-induced growth inhibition as determined by the cell cycle analysis (Fig. 4E). The fact that the majority of the cells kept proliferating for up to 16 h after FGF treatment when p107S was overexpressed indicates that overexpression of this mutant prevented FGF-induced growth arrest likely due to its ability to sequester the B55α subunit.

The inability of p107SC mutant to prevent dephosphorylation of endogenous p107 was surprising, since the affinities of both p107SC and p107S mutants for the B55α subunit were similar (Fig. 4B), as was the level of expression compared to endogenous p107. However, we noticed that p107SC protein was detected as two bands in untreated RCS cells with only one band remaining after FGF treatment. When treated with λ-phosphatase, the top band disappeared, indicating that it represented a phosphorylated form of p107SC (data not shown). Both the C terminus and the spacer region of p107 contain several phosphorylation sites: 7 in C terminus and 5 in the spacer (35). We therefore decided to check how accessible these sites were to phosphorylation using an *in*

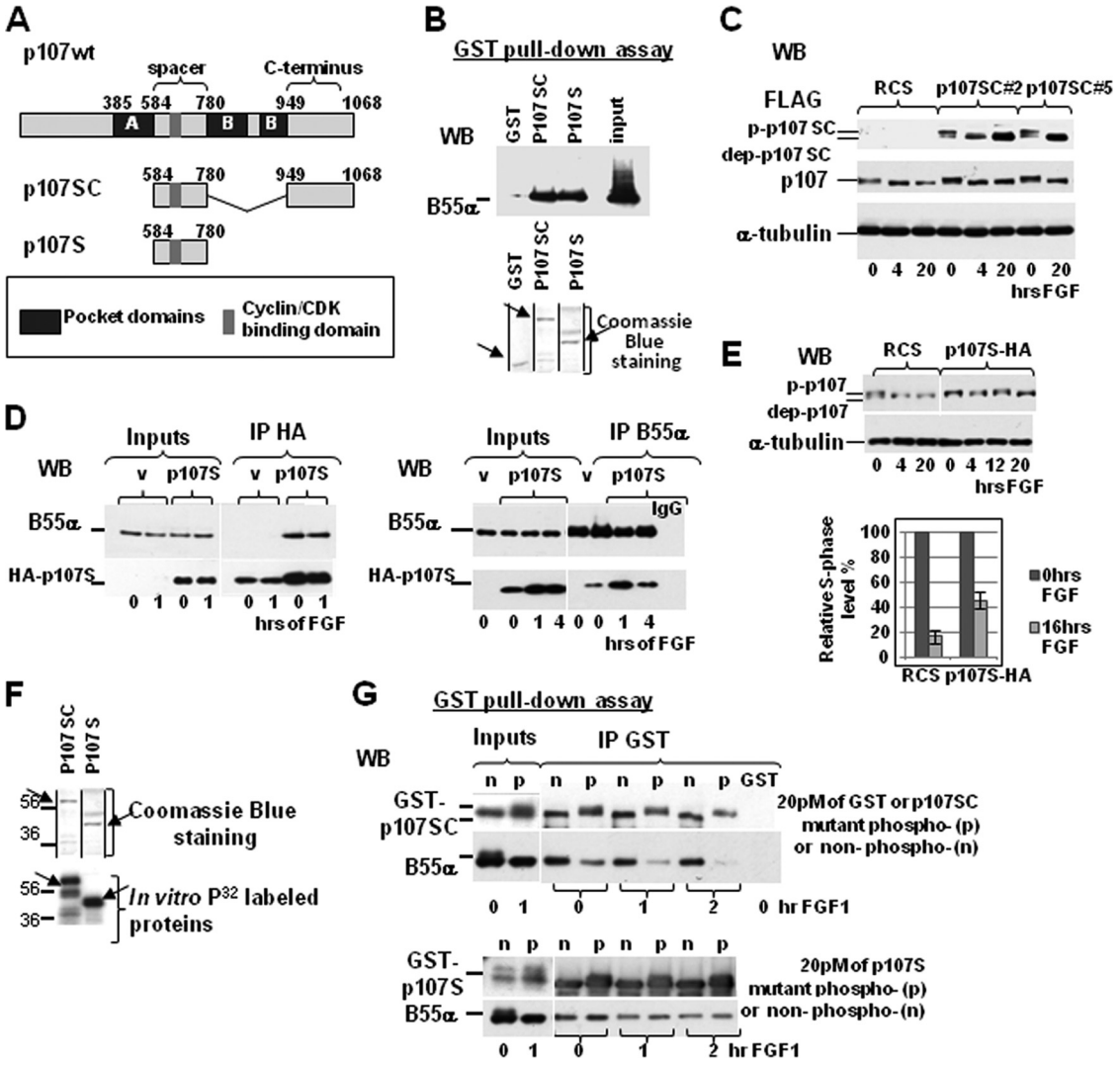

FIG 4 B55α subunit preferably binds dephosphorylated p107 through its spacer region. (A) The scheme illustrates the regions of p107 mutants purified from bacteria (B, F, and G) and overexpressed in RCS cells (C to E). Major functional domains are shown. p107wt, wild-type p107. (B) GST-p107SC (spacer fused with the C terminus) and GST-p107S (spacer) mutants, but not GST, interact with B55α in RCS cell lysates. Fifty picomoles of the proteins indicated was used in the GST pulldown assay, and the presence of B55α was assayed by immunoblotting. (C) FLAG-tagged p107SC (FLAG-p107SC) expression in RCS cells did not prevent FGF-induced p107 dephosphorylation. Ten micrograms of total protein from FGF-treated or untreated RCS cells and two different clones overexpressing FLAG-p107SC was analyzed by WB. (D and E) Overexpression of HA-tagged p107S (HA-p107S) delays FGF-induced p107 dephosphorylation and growth arrest in chondrocytes. Ten micrograms of total protein from FGF-treated or untreated cells overexpressing p107S-HA or an empty vector was analyzed by WB (E, top panel). Equal amounts of protein loading were confirmed by α-tubulin immunodetection. (D) p107S-HA interacts with endogenous B55α in RCS cells. Either p107S-HA or B55α subunit was immunoprecipitated with corresponding antibodies, and immunoprecipitated complexes were analyzed using B55α or HA antibodies as indicated. RCS cells overexpressing empty vector (v) were used as a negative control. As a reference, 5% of the immunoprecipitated whole-cell extract (input) was loaded. (E) FACScan analysis of RCS cells overexpressing p107-HA and treated with FGF for the indicated periods of time. The numbers on the *y* axis of the graph indicate the relative percentages of total cells in S phase. The data are representative of several independent experiments with similar results. (F and G) B55α subunit has higher affinity to dephosphorylated p107SC. (G) GST-p107SC and GST-p107S mutants purified from bacteria were labeled *in vitro* by cyclin E/CDK2 kinase in the presence of [γ-^{32}P]ATP, and 20 pmol of either phosphorylated or nonphosphorylated mutants were used in a GST pulldown assay with lysates from FGF-treated or untreated RCS cells. The presence of B55α was analyzed by specific antibodies, and an equal amount of the GST-p107SC mutant was confirmed by immunodetection.

vitro kinase assay. GST-tagged p107 mutants isolated from bacteria were incubated with cyclin E/CDK2 kinase in the presence of [γ-^{32}P]ATP. Both p107 mutants were efficiently phosphorylated by this p107 kinase (Fig. 4F, bottom panel). The p107SC mutant exhibited a shift in electrophoretic mobility (Fig. 4G), similar to the one we detected in p107 *in vivo* or when the same construct was overexpressed in RCS cells (Fig. 4C). Still, it was not clear why this mutant was not efficient in sequestering the B55α subunit in RCS cells. Therefore, we analyzed the interaction of phosphorylated and nonphosphorylated p107 mutants with the B55α subunit. Lysates from FGF-treated or untreated RCS cells were preincubated with equal amounts of either phosphorylated (*in vitro*) or nonphosphorylated GST-tagged p107 mutants. The results of the GST pulldown assay demonstrated that binding of B55α to the nonphosphorylated form of p107SC was much stronger (particular at later time points of FGF treatment) compared to the phos-

phorylated form (Fig. 4G). Interaction of B55α with both forms of p107SC was not increased upon FGF treatment probably due to competitive FGF-stimulated binding of endogenous p107 with B55α. This explains why the expression of p107S but not p107SC inhibited FGF-induced dephosphorylation of endogenous p107. Phosphorylation of the spacer mutant did not affect binding of B55α (Fig. 4G), and this protein was able to sequester PP2A complexes. Phosphorylated p107SC mutant was not able to compete with endogenous p107 for B55α binding and did not form enough p107SC/PP2A complexes prior to FGF treatment. The increased affinity of the B55α subunit to dephosphorylated p107 might reflect a protective mechanism that counteracts the phosphorylation of dephosphorylated p107 residues. As the binding site of B55α overlaps with identified binding sites of cyclin A/CDK2 and cyclin E/CDK2 complexes, which are also located in the spacer region of p107 (36), association with B55α could prevent interaction with p107 kinases, whose activity is downregulated by FGF at much later times (5).

Interaction of B55α with p107 is mediated by multiple interaction surfaces. Function and regulation of PP2A are in part determined by the specific regulatory B-type subunit that is present within the complex (37, 38). PP2A holoenzymes containing the B55α regulatory subunit have been implicated in the mitotic transition (14–16); several other substrates, including AKT (17), Tau protein (18), and p107 (22), were identified. An important question that has to be answered is how B55α recognizes these different substrates which show neither sequence homology nor similar pattern of dephosphorylation. Tau protein and p107, for example, are dephosphorylated at multiple sites, while in AKT and other proteins, only one residue is dephosphorylated by PP2A. To understand in more detail the interaction between p107 and B55α, we mutated several residues in this protein.

The B55α subunit is part of a family of WD40 repeat proteins, whose structure/stability depends on the presence of all WD40 repeats, thus making it complicated to localize binding sites for their partners (39). The crystal structure of the B55α subunit has been solved at 2.85-Å resolution in the context of PP2A holoenzyme (40). The B55α subunit comprises a seven-bladed β propeller, with the substrate-binding groove located in the center of the propeller. It was also shown that Glu27 and Asp197 that are located on the central groove are likely to be crucial for Tau dephosphorylation (40). p107 binding to the B55α subunit has been partially characterized in U2OS cells (22) with different conclusions about the role of Glu27 and other residues forming the substrate-binding surface. While the B55α Glu27Arg mutant was unable to dephosphorylate phospho-Tau substrate, it formed complexes with purified A and C subunits (40). When overexpressed in U2OS cells, this particular mutant retained high affinity to p107.

To determine the structural requirements of p107/B55α complexes in RCS cells, we generated a series of point mutations targeting putative substrate-binding surfaces and other elements which are accessible for binding and not involved in contacts with catalytic and scaffolding subunits or in forming WD repeats (Fig. 5A). We chose to delete Asp24-Ile30 amino acids which would eliminate Glu27 and the Lys393-Phe414 region, which is mostly unstructured with 2 very short β-sheets that are not involved in propeller formation. This region forms a loop which is oriented away from the center of the propeller and might be accessible for interaction with other proteins. For the same reason, helix α1 (Ser332-Cys341) was deleted. It is oriented perpendicular to the center of the propeller away from the blades. We also reproduce the Glu93-Lys95-to-Ala substitution and mutated Asn115-Lys117 that are close to the putative binding site to Ala as well. The later substitution would directly interfere with the putative substrate-binding surface. The proposed mutations are unlikely to change the secondary structure of B55α considerably, as they are not involved in the formation of major structural elements, such as for example any blade of the propeller.

As shown in Fig. 5B (left panel), none of the mutations affect the expression levels of either B55α or PP2A-A and C subunits (data not shown) in RCS cells. GST pulldown assay demonstrated that all the mutants were able to bind scaffolding subunit at the level comparable to that with wild-type (wt) B55α (Fig. 5B); however, the binding to PP2A-C subunit was impaired in ΔK393-F414B55α and Δhelixα1 B55α mutants. We next investigated the affinities of the mutants to p107. In p107 immunoprecipitates, wt B55α and ΔD24-I30B55α mutant were detected at similar levels (Fig. 5B, right panel), while ΔK393-F414B55α and Δhelixα1 mutants were barely detected. Mutants with affected substrate-binding groove (E93-K95→A and N115-K117→A) were still able to bind p107 though at a level lower than that of the wt protein. This difference is more noticeable when the amount of bound B55α mutants is compared to the levels of immunoprecipitated endogenous B55α (bottom bands on the B55α Western blot [WB]). Similar results were obtained when the mutants were overexpressed in 293 cells (not shown).

In summary, while p107 is likely to occupy the putative substrate-binding groove on the center surface of B55α, it makes different contacts than the Tau protein does, particularly in the region surrounding the Glu27 residue. It is interesting that the mutations in the ΔK393-F414B55α and Δhelixα1B55α mutants affected not only binding to p107 but also holoenzyme complex formation. The presence of p107 (or any other substrate) in PP2A complexes might stabilize interaction between the AC dimer and B subunit, and this stabilization likely involves ΔK393-F414 and Δhelixα1 regions. In our attempt to use helix α1 (or any other) mutant as a dominant-negative mutant and sequester the PP2A-A subunit from RCS cells, we were not able to overexpress the mutants at high enough level to compete with endogenous B55α.

B55α is dephosphorylated by FGF to target p107. From the kinetics of p107 dephosphorylation in FGF-treated chondrocytes, we would expect that FGF signaling would target the PP2A holoenzyme to increase either its affinity to p107 or the activity of the phosphatase in the already formed complexes. We were not able to detect any changes in known posttranslational modifications of the catalytic subunit, including methylation or phosphorylation upon FGF treatment. It has been demonstrated that phosphorylation of B55α at S167 is increased during mitosis and negatively affects PP2A holoenzyme formation (15). We were not able to detect such a phosphorylation event in B55α subunits in either treated or untreated cells by mass spectrometry; therefore, we decided to determine whether the B55α subunit undergoes other changes in its phosphorylation status upon FGF treatment using phospho-specific antibodies. We isolated PP2A complexes from FGF-treated or untreated cells overexpressing PR65-StrepIII subunit (Fig. 1A). No changes were detected when specific antibodies against phospho-Tyr or phospho-Thr were used (data not shown). However, phospho-pan and phospho-Ser antibodies recognized a band of the same size in untreated cells (Fig. 6A, central and right panels). The intensity of this band decreased with FGF

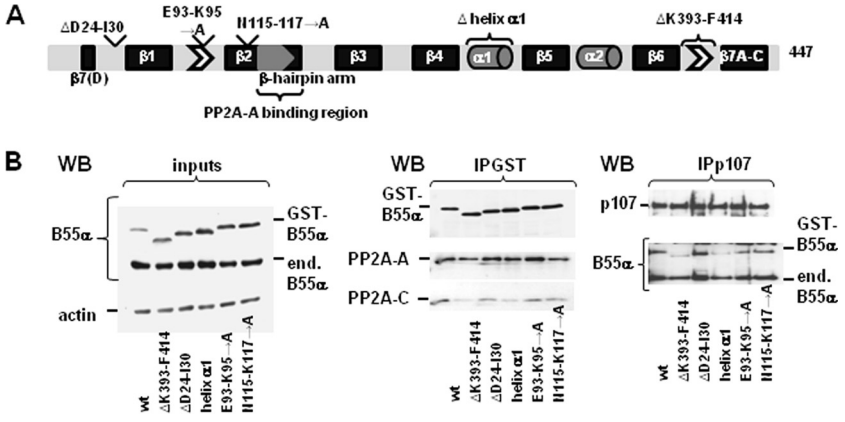

Summary of the analysis of PP2A-B55α

B55α mutants	Binding to		
	PP2A-A	PP2A-C	p107
1) wt	+++	+++	+++
2) ΔK393-F414	++	+	+
3) ΔD24-I30	+++	+++	+++
4) Δhelix α1 (S332-C341)	+++	++	+
5) E93-K95→A	+++	+++	++
6) N115-K117→A	++	++	+

FIG 5 Structural elements of the B55α subunit required for binding to p107. (A) Structural elements of the B55α subunit. The β propeller core is formed by 7 elements numbered β1 to β7. Two α-helixes (gray cylinders), β-hairpin arm (gray block arrow), and two β-sheets (white arrows) are shown. The region that makes contacts with the scaffolding subunit is indicated. Mutated residues and elements are shown above the schematic, and a summary of the results of analysis is presented in the table at the bottom of the figure. (B) GST-B55α mutants were transiently overexpressed in RCS cells (left panel). Ten micrograms of total protein was analyzed by WB using anti-B55α antibody, and equal amounts of protein loading were confirmed by α-actin immunodetection. Lysates were normalized to the amount of total protein and immunoprecipitated with either agarose-conjugated anti-GST (middle panel) or anti-p107 antibodies (right panel). The presence of the indicated proteins was assayed by immunoblotting. Anti-B55α antibody was used to detect both GST-tagged and endogenous (end.) protein. The table represents summary of the analysis of PP2A-B55a mutants. +++, strong binding; ++, moderate binding; +, weak binding.

treatment. This band coincided with the band recognized by B55α-specific antibodies, and when analyzed by mass spectrometry, it was primarily assigned to B55α. To confirm that FGF induces dephosphorylation of B55α, we immunoprecipitated the B55α subunit from denatured lysates, so that anti-B55α antibodies immunoprecipitate only B55α without any associated proteins that could influence its phosphorylation status. As shown in Fig. 6B, the signal corresponding to ^{32}P-labeled B55α immunoprecipitated from metabolically labeled RCS cells declines significantly with FGF treatment. In line with these data, FGF-induced decrease in B55α phosphorylation was clearly detected when using anti-phospho-pan antibodies (Fig. 6C). To support our findings, we assayed the phosphorylation status of the B55α subunit in p107 immunoprecipitates. The amount of B55α associated with p107 was increased with FGF treatment, but no phosphorylated B55α was detected as assayed by phospho-pan (Fig. 6D) or phospho-Ser antibodies (data not shown). This result suggests that FGF-induced dephosphorylation of B55α might increase the affinity of PP2A to p107 and/or directly affect PP2A activity. Therefore, we analyzed the effects of phospho-mimicking (Ser→Glu) or nonphosphorylated (Ser→Ala) mutations of serine residues on the ability of B55α to support PP2A holoenzyme formation and to bind p107.

Ser residues that had a score of at least 0.8 according to NetPhos 2.0 prediction results (41) and were conserved between known mammalian sequences were selected to be mutated.

The mutants (Fig. 7A and PP2A-B55a Ser mutation table) were transiently overexpressed in RCS cells, and their ability to associate with the PP2A-A subunit and p107 was examined. None of the mutations affect the level of overexpressed B55α subunits (Fig. 7B and C). According to the ability to form complexes with the scaffolding subunit, the mutants have been divided in three groups: no effect (S400 [Fig. 7B]), effect independent on phosphorylation status (Ser187, Ser194, and Ser246 [Fig. 7C]) and effect dependent of phosphorylation status (Ser125, Ser266, and Ser294 [Fig. 7B and C and table]). While the mutated residues in the second group are likely to affect protein conformation or function, the results with the third group strongly suggest that phosphorylation of specific Ser residues interferes with the ability of B55α to form stable trimeric complexes and to interact with p107, in agreement with the results showing that p107 preferentially binds to dephosphorylated B55α. The mutants that formed a complex with the PP2A-A subunit were also able to bind p107 with the exception of the S294A mutant, which was able to bind to the scaffolding subunit, but no p107 was detected in its immunoprecipitates (Fig. 7C). In general, the ability of the mutants to bind to p107 mimicked the ability of the mutants to form PP2A holoenzymes, implying that in chondrocytes, the B55α regulatory subunit mediates

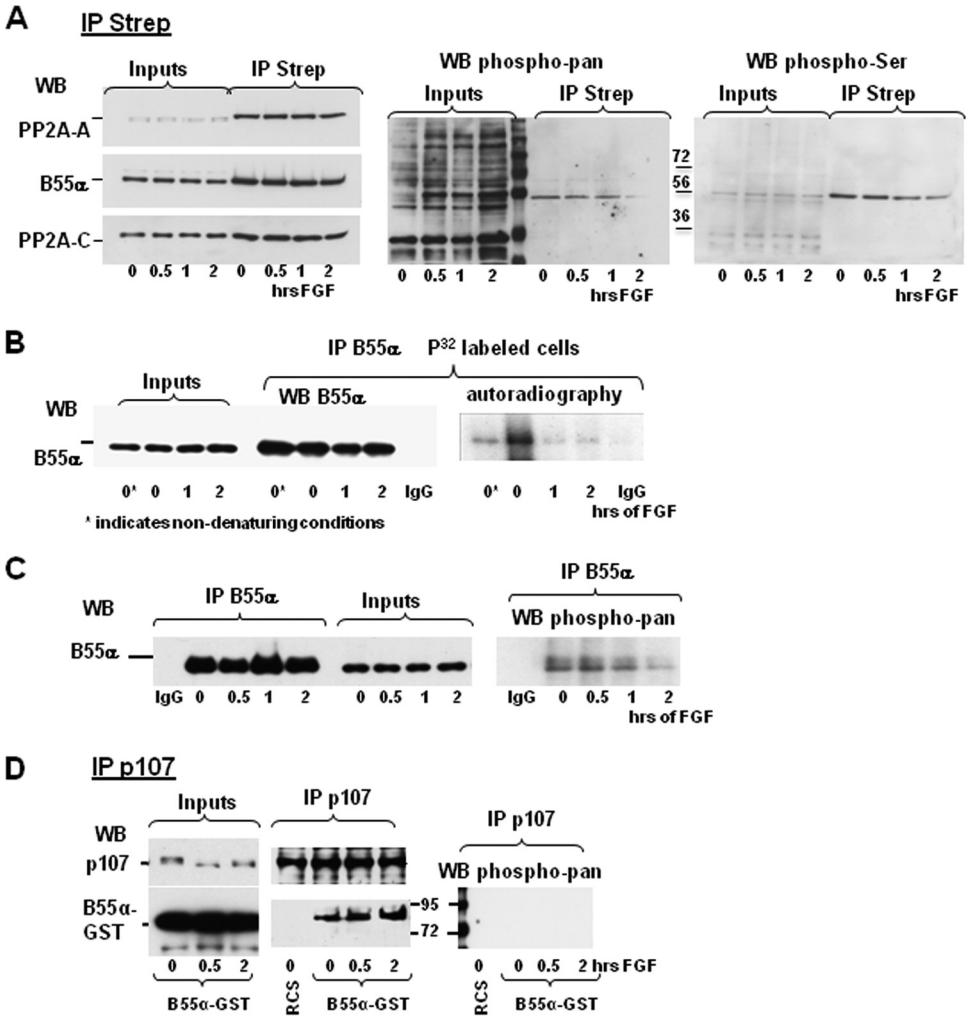

FIG 6 Dephosphorylation of B55α is induced upon FGF treatment in chondrocytes. (A) PR65-StrepIII (subunit A, a scaffolding subunit) was stably introduced into RCS cells, and these cells were treated with FGF for the indicated periods of time (in hours). Lysates were normalized to the amount of total protein and immunoprecipitated on a Strep-Tactin column. As a reference, 5% of the immunoprecipitated whole-cell extract (input) was loaded. The presence of indicated proteins was assayed either by anti-PP2A-A, anti-B55α, and anti-PP2A-C antibodies (left panel) or by pan-phospho-Tyr/Ser/Thr antibodies (central and right panels). (B and C) FGF-induced dephosphorylation of the B55α subunit. B55α was immunoprecipitated from FGF-treated RCS cells ^{32}P metabolically labeled (B) or not metabolically labeled (C) under denaturing conditions (0.3% SDS). Lysates were normalized to the amount of total protein, and the presence of B55α was assayed by immunoblotting. The phosphorylation status of B55α was assayed either by autoradiography (B, right panel) or by anti-phospho-pan antibodies (C, right panel). (D) The B55α subunit bound to p107 is not phosphorylated. The GST-B55α subunit was overexpressed in RCS cells, and following FGF treatment, lysates were immunoprecipitated using agarose-conjugated p107 antibody. As a reference, 5% of the immunoprecipitated whole-cell extract (input) was loaded. The presence of indicated proteins was assayed by anti-p107 and anti-B55α antibodies (left and central panels). There was no detectable signal when phospho-pan antibody was used (right panel). The stained bands correspond to protein markers (72 and 95 kDa) that are routinely recognized by phospho-pan antibodies.

substrate recognition in the context of trimeric PP2A complexes. FGF-induced dephosphorylation of B55α could target any of the these Ser residues, and the mechanism of this dephosphorylation remains to be elucidated. This can involve either another Ser/Thr phosphatase (for example, PP1) or be mediated by PP2A itself, whose autodephosphorylation ability has been reported previously (42).

FGF sensitivity of B55α/p107 interaction is RCS specific. The inhibition of chondrocyte proliferation induced by FGF is a cell type-specific response that contrasts with the proliferative FGF response in most other cells. We have shown that p107 dephosphorylation is a key event in mediating FGF-induced growth arrest in chondrocytes (27). Taking into account the fact that p107/B55α interaction was detected in other cell lines (22), we wished to understand whether the increased affinity of p107 and B55α upon FGF treatment is cell type specific and unique to cells where FGF induces cell cycle arrest. Two cell lines were chosen for this experiment, both exhibiting proliferative response to FGF: OB1 osteoblastic cell line (43) and $C_3H_{10}T1/2$ multipotential mesenchymal cells that can be differentiated into the chondrogenic lineage (44). As shown in Fig. 8 (left panel), while FGF caused ERK activation in all three cell lines, p107 was rapidly dephosphorylated only in RCS cells. Moreover, when B55α immunoprecipitates were analyzed for the presence of p107, only RCS cells exhibited a strong increase in binding of B55α to p107 upon FGF treatment (Fig. 8, right

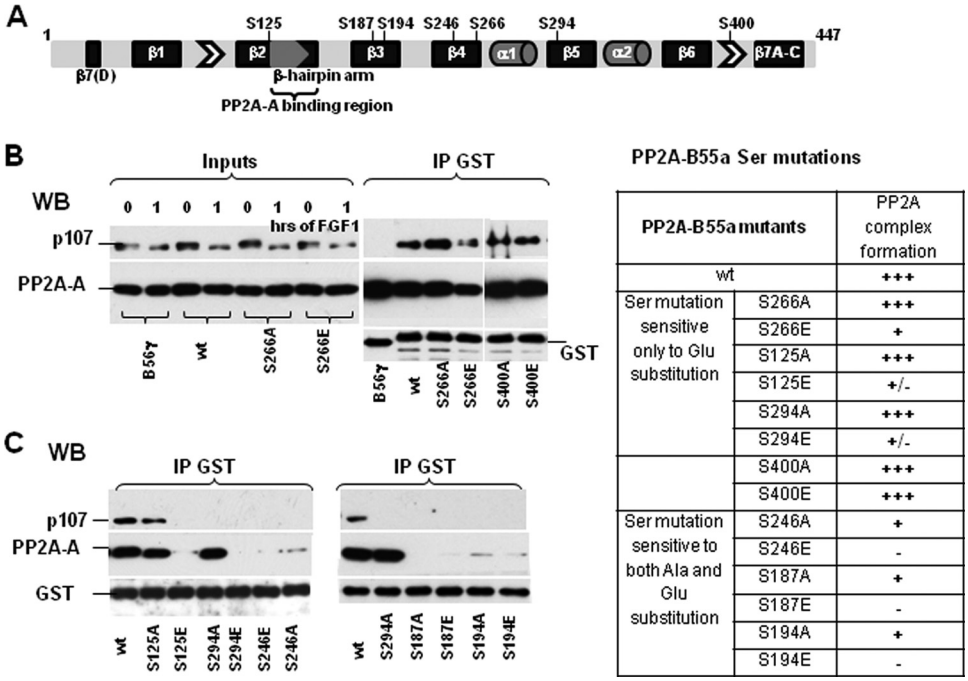

PP2A-B55a Ser mutations

PP2A-B55a mutants		PP2A complex formation
wt		+++
Ser mutation sensitive only to Glu substitution	S266A	+++
	S266E	+
	S125A	+++
	S125E	+/-
	S294A	+++
	S294E	+/-
	S400A	+++
	S400E	+++
Ser mutation sensitive to both Ala and Glu substitution	S246A	+
	S246E	-
	S187A	+
	S187E	-
	S194A	+
	S194E	-

FIG 7 Dephosphorylation of B55α is important for the stability of PP2A-B55α holoenzymes and binding to p107. (A) Structural elements of the B55α subunit. The β propeller core is formed by 7 elements numbered β1 to β7. Two α-helixes (gray cylinders), β-hairpin arm (gray block arrow), and two β-sheets (white arrows) are shown. The region that makes contacts with the scaffolding subunit is indicated. Mutated Ser residues are shown above the schematic. (B and C) GST-B55α mutants were transiently overexpressed in RCS cells. Lysates from FGF-treated or untreated cells were normalized by the amount of total protein and immunoprecipitated with anti-GST antibodies. As a reference, 5% of the immunoprecipitated whole-cell extract (input) was loaded (shown for several proteins and similar for all mutants). The presence of GST-B55α mutants, PP2A-A subunit, and p107 was assayed by corresponding antibodies. RCS cells overexpressing B56γ subunit were used as a negative control. PP2A complex formation is shown in the table to the right of panels B and C. The ability of PP2A-B55a mutants to support PP2A trimeric complex formation is summarized in the table: −, no complexes formed; +/−, very weak binding; +, weak binding; +++, strong binding.

panel). Thus, the FGF sensitivity of B55α/p107 complexes is chondrocyte specific and probably plays an important role in the FGF inhibitory response of these cells.

DISCUSSION

p107 dephosphorylation is an early and key event in mediating the FGF inhibitory response in chondrocytes (27). While phosphorylation of p107 and the other Rb proteins is extensively studied and fairly well understood, the mechanism of pocket protein dephosphorylation/activation remains to be elucidated both during the cell cycle and under different stress conditions (35). Understanding this mechanism will provide significant insight into general regulation of Rb proteins and also facilitate understanding the unique chondrocyte-specific FGF inhibitory response. We previously showed that the PP2A phosphatase mediates FGF-induced p107 dephosphorylation, but the regulatory subunit that targets

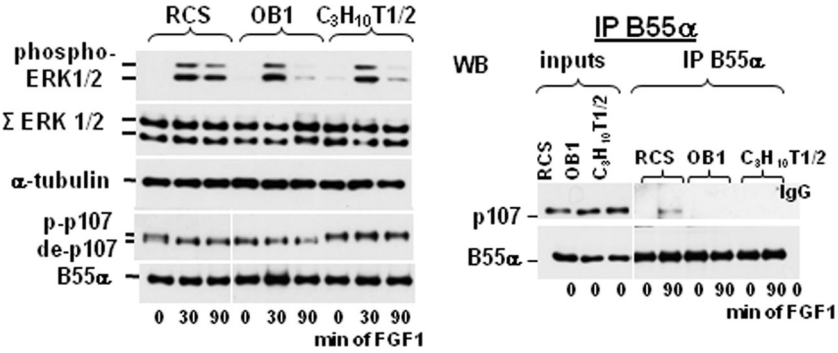

FIG 8 The induction of B55α/p107 interaction by FGF is cell type specific. FGF causes ERK1/2 activation in the cell lines with both a proliferative response (OB1 and $C_3H_{10}T1/2$ cells) and an inhibitory response (RCS cells). Twenty micrograms of total protein from the indicated cell lines treated with FGF or not treated with FGF was analyzed by SDS-PAGE, followed by immunoblotting with anti-phospho-ERK1/2, anti-ERK1/2, p107, and B55α antibodies. (Left) Equal amounts of protein loading were confirmed by α-tubulin immunodetection. Lysates from FGF-treated or untreated cells were normalized by the amount of total protein and immunoprecipitated with anti-B55α antibodies. As a reference, 5% of the immunoprecipitated whole-cell extract (input) was loaded. The presence of p107 in B55α IP was assayed by immunodetection.

PP2A to p107 in chondrocytes was not identified. In this work, we demonstrate that the B55α regulatory subunit of PP2A specifically interacts with p107 in an FGF-dependent manner and that this interaction is important for FGF-mediated inhibition of chondrocyte proliferation. Immunoprecipitation of either protein detected the other protein in the same complex. Downregulation of B55α by siRNA resulted in delayed FGF-induced p107 dephosphorylation and resistance to FGF-induced growth arrest, supporting the hypothesis that the PP2A-B55α holoenzyme mediates this process.

While the B55α/p107 interaction is preserved in many other cell lines (U2OS [22], RCS, OB1, 293, $C_3H_{10}T1/2$, and primary chondrocytes [this study]), it is stimulated by FGF only in chondrocytes, underlining the importance of p107 dephosphorylation for FGF-induced growth arrest. The ability of the B55α regulatory subunit to bind p107 in many different systems suggests that the same PP2A-B55α holoenzyme mediates p107 dephosphorylation during the cell cycle and when rapid dephosphorylation is dictated by external stress or growth inhibitory signals. It would be interesting to see whether the interaction between B55α and p107 is altered as cells progress through the cell cycle and how important this interaction is for progression through the different phases of the cell cycle. It has also been demonstrated that the B55α subunit is a key player in mitotic spindle breakdown and postmitotic reassembly of the nuclear envelope and Golgi apparatus (15). Thus, the activity of the PP2A-B55α holoenzyme could be regulated to dephosphorylate diverse targets during the cell cycle and under growth inhibitory conditions. Additional PP2A holoenzymes might also be regulated during the cell cycle in a similar or different manner because other important cell cycle players such as, for example, p27 are also regulated by PP2A (45).

In agreement with previously published data (22), we found that the spacer region of p107 was alone sufficient to bind B55α. As expected, overexpression of this domain was able to counteract FGF-induced p107 dephosphorylation and growth arrest in RCS cells, supporting the notion that trapping of B55α was sufficient to inhibit targeting of PP2A to p107.

We reported previously that not only p107 but also the p130 Rb protein is an essential mediator of FGF-induced growth arrest in chondrocytes (2). However, in contrast to the data obtained with U2OS cells (22), we were not able to detect any interaction between B55α and p130 in FGF-treated or untreated RCS cells. The reason for the discrepancy in p130/B55α interaction might be due to the diverse context of p130/PP2A interaction in U2OS cells, as p130 appears to be less selective than p107 and can interact with other members of the regulatory subunit families, such as PR70. Furthermore, p130 is dephosphorylated at much later times after FGF treatment than p107, and thus, it is likely that inactivation of CDKs would be as important for p130 dephosphorylation as the activation of a specific phosphatase. The PR48 subunit (truncated version of PR70) was also reported to bind p107 (22); however, we were not able to detect this subunit in RCS cells by using the appropriate antibodies or in PP2A complexes by mass spectrometry.

An intriguing observation is the difference in the affinity of B55α to phosphorylated and nonphosphorylated p107SC mutant, whose phosphorylation either *in vitro* or *in vivo* (Fig. 4) mimics phosphorylation of the endogenous p107. While the higher affinity of B55α to nonphosphorylated protein seems to be counterintuitive, p107 is not the only PP2A-B55α substrate which behaves in this manner. It has been shown that a synthetic peptide corresponding to the region of Tau protein that binds to B55α was able to compete with full-length Tau protein for B55α, while its phosphorylated analogue was not (46). This particular region is also recognized by the Fyn kinase, which has been implicated in Tau phosphorylation (46). Another example of a phosphatase/kinase overlapping binding site is the C terminus of Rb, which contains the PP1 docking site and the binding site for CDKs (47). In our case, increased binding of B55α to dephosphorylated p107 might protect it from phosphorylation by the CDKs, such as the cyclin D/CDK4, cyclin E/CDK2, or cyclin A/CDK2 complexes, as all these complexes bind to p107 through the spacer region, which contains the cyclin-binding RXL motif (48). Such protection may be important to sustain FGF-induced p107 dephosphorylation, since CDK activity is inhibited at later times of FGF treatment (2). The ability of the PP2A phosphatase and CDKs to compete for the same p107 region suggests a dynamic equilibrium between these counteracting enzymes during the cell cycle (49). Indeed, our results and those of Jayadeva (22) suggest that the B55α-containing PP2A holoenzyme would also be responsible for the dephosphorylation of p107 in the cell cycle.

B55α is one of the most abundant regulatory subunits of PP2A and has been implicated in many diverse functions of the phosphatase. Many different substrates have been reported for PP2A-B55α holoenzymes, including cyclin B1/CDK1 substrates (15), Tau protein (40), β-catenin (21), FoxM1 transcription factor (50), as well as p107 (22). It is still not clear how B55α targets all these different substrates, as these proteins have nothing in common. According to our data, B55α can discriminate between different substrates utilizing distinct contacts in the context of an acidic, substrate-binding groove. For example, the residues important for Tau protein dephosphorylation (Glu93-Lys95 and Glu27) are dispensable for binding p107, as the corresponding mutations had no effect on p107/B55α complex formation (40). On the other hand, two structural elements of B55α (helix α1 and β2 hairpin), which are not involved in the formation of WD repeats, affected both association with p107 and (for β2 hairpin mutant) binding to A/C dimer. These regions probably contribute to the formation of the substrate-binding groove. It would be interesting to see whether these mutations affect binding of other substrates as well.

p107/B55α complexes accumulate upon FGF treatment in chondrocytes, and while a higher affinity of B55α to dephosphorylated p107 could be partially responsible for this accumulation, an event initiated by FGF signaling would seem necessary to "activate" PP2A and to induce p107 dephosphorylation. Our data suggest that this activation consists of dephosphorylation of the B55α subunit. We showed by immunoprecipitating B55α from ^{32}P-labeled cells that the protein is dephosphorylated with kinetics similar to the kinetics of FGF-induced p107 dephosphorylation, and we obtained similar results using phospho-pan antibodies. We also demonstrated by using either phospho-mimicking or nonphosphorylated substitutions that when phosphorylated at any of the serine residues at position 125, 266, or 294, B55α was unable to form stable complexes with A subunit. Interestingly, the S266E B55α mutant still exhibited a modest ability to bind the scaffolding subunit, indicating that FGF-induced dephosphorylation of the B55α subunit might be differential. Clearly, all three residues have to be dephosphorylated to provide maximum stability/activity to the PP2A-B55α holoenzyme and to fulfill PP2A

functions in mediating FGF-induced growth arrest. We were not able to detect any phosphorylation of S167, which has been shown to affect PP2A-B55α function during mitotic transition (15), suggesting that this subunit may be regulated differently for different substrates. At present, the phosphatase that is responsible for B55α dephosphorylation (as well as the kinase responsible for its phosphorylation) is not known; however, it is unlikely that this phosphatase is PP2A itself, as we did not detect any FGF-induced posttranslational modifications of either scaffolding or catalytic subunits. FGF is known to activate Shp2, which is however a tyrosine phosphatase and thus unlikely to dephosphorylate B55α. Rather, another Ser/Thr phosphatase (for example, PP1) might be responsible for this activation. In conclusion, our results identify the PP2A-B55α holoenzyme as a crucial mediator of the chondrocyte FGF growth inhibitory response. FGF signaling activates the phosphatase through dephosphorylation of its regulatory subunit to mediate p107 activation. We are currently investigating the mechanism of this novel aspect of FGF signaling to understand PP2A regulation as well as cell type-specific mechanisms that distinguish the FGF response of chondrocytes from those of other cell types.

ACKNOWLEDGMENTS

We thank J. Kraynak for help with some of the experiments, Xavier Grana and Jukka Westermarck for helpful discussions, and Upal Basu Roy for critical reading of the manuscript. We are grateful to Veerle Janssens, David Virshup, Xavier Grana, and Jukka Westermarck for providing plasmids.

This investigation was supported in part by PHS grant DE013745 from the NIDCR and by a postdoctoral fellowship from the NCI training grant T32 CA009161 to V.K.

REFERENCES

1. **Aviezer D, Golembo M, Yayon A.** 2003. Fibroblast growth factor receptor-3 as a therapeutic target for achondroplasia–genetic short limbed dwarfism. Curr. Drug Targets **4:**353–365.
2. **Laplantine E, Rossi F, Sahni M, Basilico C, Cobrinik D.** 2002. FGF signaling targets the pRb-related p107 and p130 proteins to induce chondrocyte growth arrest. J. Cell Biol. **158:**741–750.
3. **Cobrinik D, Lee MH, Hannon G, Mulligan G, Bronson RT, Dyson N, Harlow E, Beach D, Weinberg RA, Jacks T.** 1996. Shared role of the pRB-related p130 and p107 proteins in limb development. Genes Dev. **10:**1633–1644.
4. **Dyson N.** 1998. The regulation of E2F by pRB-family proteins. Genes Dev. **12:**2245–2262.
5. **Dailey L, Laplantine E, Priore R, Basilico C.** 2003. A network of transcriptional and signaling events is activated by FGF to induce chondrocyte growth arrest and differentiation. J. Cell Biol. **161:**1053–1066.
6. **Aikawa T, Segre GV, Lee K.** 2001. Fibroblast growth factor inhibits chondrocytic growth through induction of p21 and subsequent inactivation of cyclin E-Cdk2. J. Biol. Chem. **276:**29347–29352.
7. **Janssens V, Longin S, Goris J.** 2008. PP2A holoenzyme assembly: in cauda venenum (the sting is in the tail). Trends Biochem. Sci. **33:**113–121.
8. **Janssens V, Rebollo A.** 2012. The role and therapeutic potential of Ser/Thr phosphatase PP2A in apoptotic signalling networks in human cancer cells. Curr. Mol. Med. **12:**268–287.
9. **Kalev P, Sablina AA.** 2011. Protein phosphatase 2A as a potential target for anticancer therapy. Anticancer Agents Med. Chem. **11:**38–46.
10. **Kalev P, Simicek M, Vazquez I, Munck S, Chen L, Soin T, Danda N, Chen W, Sablina A.** 2012. Loss of PPP2R2A inhibits homologous recombination DNA repair and predicts tumor sensitivity to PARP inhibition. Cancer Res. **72:**6414–6424.
11. **Westermarck J, Hahn WC.** 2008. Multiple pathways regulated by the tumor suppressor PP2A in transformation. Trends Mol. Med. **14:**152–160.
12. **Junttila MR, Puustinen P, Niemela M, Ahola R, Arnold H, Bottzauw T, Ala-aho R, Nielsen C, Ivaska J, Taya Y, Lu SL, Lin S, Chan EK, Wang XJ, Grenman R, Kast J, Kallunki T, Sears R, Kahari VM, Westermarck J.** 2007. CIP2A inhibits PP2A in human malignancies. Cell **130:**51–62.
13. **Sablina AA, Hahn WC.** 2008. SV40 small T antigen and PP2A phosphatase in cell transformation. Cancer Metastasis Rev. **27:**137–146.
14. **Gharbi-Ayachi A, Labbe JC, Burgess A, Vigneron S, Strub JM, Brioudes E, Van-Dorsselaer A, Castro A, Lorca T.** 2010. The substrate of Greatwall kinase, Arpp19, controls mitosis by inhibiting protein phosphatase 2A. Science **330:**1673–1677.
15. **Schmitz MH, Held M, Janssens V, Hutchins JR, Hudecz O, Ivanova E, Goris J, Trinkle-Mulcahy L, Lamond AI, Poser I, Hyman AA, Mechtler K, Peters JM, Gerlich DW.** 2010. Live-cell imaging RNAi screen identifies PP2A-B55alpha and importin-beta1 as key mitotic exit regulators in human cells. Nat. Cell Biol. **12:**886–893.
16. **Wurzenberger C, Gerlich DW.** 2011. Phosphatases: providing safe passage through mitotic exit. Nat. Rev. Mol. Cell Biol. **12:**469–482.
17. **Kuo YC, Huang KY, Yang CH, Yang YS, Lee WY, Chiang CW.** 2008. Regulation of phosphorylation of Thr-308 of Akt, cell proliferation, and survival by the B55alpha regulatory subunit targeting of the protein phosphatase 2A holoenzyme to Akt. J. Biol. Chem. **283:**1882–1892.
18. **Voronkov M, Braithwaite SP, Stock JB.** 2011. Phosphoprotein phosphatase 2A: a novel druggable target for Alzheimer's disease. Future Med. Chem. **3:**821–833.
19. **Yan L, Guo S, Brault M, Harmon J, Robertson RP, Hamid R, Stein R, Yang E.** 2012. The B55alpha-containing PP2A holoenzyme dephosphorylates FOXO1 in islet beta-cells under oxidative stress. Biochem. J. **444:**239–247.
20. **Reid MA, Wang WI, Rosales KR, Welliver MX, Pan M, Kong M.** 2013. The B55alpha subunit of PP2A drives a p53-dependent metabolic adaptation to glutamine deprivation. Mol. Cell **50:**200–211.
21. **Zhang W, Yang J, Liu Y, Chen X, Yu T, Jia J, Liu C.** 2009. PR55 alpha, a regulatory subunit of PP2A, specifically regulates PP2A-mediated beta-catenin dephosphorylation. J. Biol. Chem. **284:**22649–22656.
22. **Jayadeva G, Kurimchak A, Garriga J, Sotillo E, Davis AJ, Haines DS, Mumby M, Grana X.** 2010. B55alpha PP2A holoenzymes modulate the phosphorylation status of the retinoblastoma-related protein p107 and its activation. J. Biol. Chem. **285:**29863–29873.
23. **Voorhoeve PM, Hijmans EM, Bernards R.** 1999. Functional interaction between a novel protein phosphatase 2A regulatory subunit, PR59, and the retinoblastoma-related p107 protein. Oncogene **18:**515–524.
24. **Raucci A, Laplantine E, Mansukhani A, Basilico C.** 2004. Activation of the ERK1/2 and p38 mitogen-activated protein kinase pathways mediates fibroblast growth factor-induced growth arrest of chondrocytes. J. Biol. Chem. **279:**1747–1756.
25. **Thirion S, Berenbaum F.** 2004. Culture and phenotyping of chondrocytes in primary culture. Methods Mol. Med. **100:**1–14.
26. **Longin S, Zwaenepoel K, Louis JV, Dilworth S, Goris J, Janssens V.** 2007. Selection of protein phosphatase 2A regulatory subunits is mediated by the C terminus of the catalytic subunit. J. Biol. Chem. **282:**26971–26980.
27. **Kolupaeva V, Laplantine E, Basilico C.** 2008. PP2A-mediated dephosphorylation of p107 plays a critical role in chondrocyte cell cycle arrest by FGF. PLoS One **3:**e3447. doi:10.1371/journal.pone.0003447.
28. **Browne GJ, Proud CG.** 2002. Regulation of peptide-chain elongation in mammalian cells. Eur. J. Biochem. **269:**5360–5368.
29. **Kaul G, Pattan G, Rafeequi T.** 2011. Eukaryotic elongation factor-2 (eEF2): its regulation and peptide chain elongation. Cell Biochem. Funct. **29:**227–234.
30. **Lin KW, Yakymovych I, Jia M, Yakymovych M, Souchelnytskyi S.** 2010. Phosphorylation of eEF1A1 at Ser300 by TbetaR-I results in inhibition of mRNA translation. Curr. Biol. **20:**1615–1625.
31. **Ryazanov AG.** 2002. Elongation factor-2 kinase and its newly discovered relatives. FEBS Lett. **514:**26–29.
32. **Tsuchiya Y, Denison FC, Heath RB, Carling D, Saggerson D.** 2012. 5′-AMP-activated protein kinase is inactivated by adrenergic signalling in adult cardiac myocytes. Biosci. Rep. **32:**197–213.
33. **Papakonstanti EA, Stournaras C.** 2002. Association of PI-3 kinase with PAK1 leads to actin phosphorylation and cytoskeletal reorganization. Mol. Biol. Cell **13:**2946–2962.
34. **Rozenblatt-Rosen O, Mosonego-Ornan E, Sadot E, Madar-Shapiro L, Sheinin Y, Ginsberg D, Yayon A.** 2002. Induction of chondrocyte growth arrest by FGF: transcriptional and cytoskeletal alterations. J. Cell Sci. **115:**553–562.

35. **Kolupaeva V, Janssens V.** 2013. PP1 and PP2A phosphatases – cooperating partners in modulating retinoblastoma protein activation. FEBS J. **280:**627–643.
36. **Woo MS, Sanchez I, Dynlacht BD.** 1997. p130 and p107 use a conserved domain to inhibit cellular cyclin-dependent kinase activity. Mol. Cell. Biol. **17:**3566–3579.
37. **Shi Y.** 2009. Serine/threonine phosphatases: mechanism through structure. Cell **139:**468–484.
38. **Slupe AM, Merrill RA, Strack S.** 2011. Determinants for substrate specificity of protein phosphatase 2A. Enzyme Res. **2011:**398751. doi:10.4061/2011/398751.
39. **Xu C, Min J.** 2011. Structure and function of WD40 domain proteins. Protein Cell **2:**202–214.
40. **Xu Y, Chen Y, Zhang P, Jeffrey PD, Shi Y.** 2008. Structure of a protein phosphatase 2A holoenzyme: insights into B55-mediated Tau dephosphorylation. Mol. Cell **31:**873–885.
41. **Blom N, Gammeltoft S, Brunak S.** 1999. Sequence and structure-based prediction of eukaryotic protein phosphorylation sites. J. Mol. Biol. **294:**1351–1362.
42. **Fukunaga K, Muller D, Ohmitsu M, Bako E, DePaoli-Roach AA, Miyamoto E.** 2000. Decreased protein phosphatase 2A activity in hippocampal long-term potentiation. J. Neurochem. **74:**807–817.
43. **Mansukhani A, Bellosta P, Sahni M, Basilico C.** 2000. Signaling by fibroblast growth factors (FGF) and fibroblast growth factor receptor 2 (FGFR2)-activating mutations blocks mineralization and induces apoptosis in osteoblasts. J. Cell Biol. **149:**1297–1308.
44. **Denker AE, Haas AR, Nicoll SB, Tuan RS.** 1999. Chondrogenic differentiation of murine C3H10T1/2 multipotential mesenchymal cells. I. Stimulation by bone morphogenetic protein-2 in high-density micromass cultures. Differentiation **64:**67–76.
45. **Miller JP, Yeh N, Hofstetter CP, Keskin D, Goldstein AS, Koff A.** 2012. p27kip1 protein levels reflect a nexus of oncogenic signaling during cell transformation. J. Biol. Chem. **287:**19775–19785.
46. **Sontag JM, Nunbhakdi-Craig V, White CL, III, Halpain S, Sontag E.** 2012. The protein phosphatase PP2A/Balpha binds to the microtubule-associated proteins Tau and MAP2 at a motif also recognized by the kinase Fyn: implications for tauopathies. J. Biol. Chem. **287:**14984–14993.
47. **Hirschi A, Cecchini M, Steinhardt RC, Schamber MR, Dick FA, Rubin SM.** 2010. An overlapping kinase and phosphatase docking site regulates activity of the retinoblastoma protein. Nat. Struct. Mol. Biol. **17:**1051–1057.
48. **Castano E, Kleyner Y, Dynlacht BD.** 1998. Dual cyclin-binding domains are required for p107 to function as a kinase inhibitor. Mol. Cell. Biol. **18:**5380–5391.
49. **Garriga J, Jayaraman AL, Limon A, Jayadeva G, Sotillo E, Truongcao M, Patsialou A, Wadzinski BE, Grana X.** 2004. A dynamic equilibrium between CDKs and PP2A modulates phosphorylation of pRB, p107 and p130. Cell Cycle **3:**1320–1330.
50. **Alvarez-Fernandez M, Halim VA, Aprelia M, Laoukili J, Mohammed S, Medema RH.** 2011. Protein phosphatase 2A (B55alpha) prevents premature activation of forkhead transcription factor FoxM1 by antagonizing cyclin A/cyclin-dependent kinase-mediated phosphorylation. J. Biol. Chem. **286:**33029–33036.
51. **Junttila MR, Saarinen S, Schmidt T, Kast J, Westermarck J.** 2005. Single-step Strep-tag purification for the isolation and identification of protein complexes from mammalian cells. Proteomics **5:**1199–1203.